Surface effects and structural dependence of magneto-optical spectra: Ultrathin Co films and $CoPt_n$ alloys and multilayers

Miyoung Kim and A. J. Freeman
Department of Physics and Astronomy, Northwestern University, Evanston, Illinois 60208-3112

Ruqian Wu
Department of Physics and Astronomy, California State University, Northridge, California 91330-8268

(Received 7 August 1998)

First-principles calculations of the optical conductivities and magneto-optical Kerr effects for bulk and thin films of Co and for $CoPt_n$ alloys ($n=1$ and 3) and multilayer ($n=3$) are carried out using the full potential linearized augmented plane wave method with the local spin density approximation. For fcc bulk Co, we obtain a negligible dependence of the polar Kerr rotation on the direction of magnetization. By contrast, the calculated Kerr spectra of $CoPt_n$ are found to be very sensitive to structural changes. For Co(001) and Co(111) ultrathin films, the surface effects cause a redshift for the high-energy peaks in the magneto-optic Kerr effect (MOKE) spectra, mainly due to band narrowing. Except for the free standing Co(001) monolayer, the profile of their MOKE spectra, however, is very close to that of bulk Co. [S0163-1829(99)04313-1]

I. INTRODUCTION

The surface magneto-optical Kerr effect (SMOKE) has been used as an essential tool for *in situ* investigations of surface magnetism in recent years.[1] Also, spurred by its potential application in high density optical storage media, a great number of magneto-optic experiments for various materials have been performed aiming at the fabrication of materials exhibiting desired magneto-optical properties.[2] Following the early work by Argyres,[3] Bennett and Stern,[4] and later by Callaway and Wang,[5] theoretical studies of MOKE based on modern local spin density functional electronic structure approaches have made significant progress in the last few years. Both optical conductivities and MOKE spectra can be directly determined by first-principles calculations with an impressive accuracy compared to experiment. Many metals and metal compounds have been investigated theoretically[6] not only to predict magneto-optical materials not yet been made experimentally but also to provide better explanations for the experimental results.

Recently, extensive studies of Fe, Co, and Ni systems discovered that their MOKE spectra depend sensitively on many factors such as lattice size, exchange splitting, spin-orbit coupling, orbital magnetic moment and even the orientation of the magnetization.[7–10] This paper reports results of our first-principles investigations for the MOKE spectra of Co in various environments, e.g., fcc bulk Co, Co(001), and Co(111) surfaces and CoPt compounds. The calculated MOKE spectra for fcc bulk Co are found to be almost identical when the magnetization points along the (001) and (111) directions, which confirms the conclusion obtained previously from both calculations[8,9] and experiments[11] for fcc bulk Co with the magnetization along the (001) and (110) directions. For the free standing fcc Co ultrathin films, the optical conductivities and MOKE spectra depend sensitively on the thickness—indicating the presence of strong surface and quantum confinement effects.

II. METHODOLOGY

For the first-principles electronic structure calculations, we employed the full potential linearized augmented plane wave (FLAPW) method[12] without any artificial shape approximation for the wave functions, charge density, and potential. The core states are treated fully relativistically and the valence states are treated scalar-relativistically within the framework of the local spin density approximation (LSDA). The spin-orbit coupling (SOC) part is invoked in a second variational way.[13] Using the FLAPW wave functions and energy eigenvalues, the elements of the optical conductivity tensor due to the interband transitions are calculated with the linear response theory—by solving Kubo's formula for the current response to the time-dependent external field. The diagonal and off-diagonal conductivities are given by[14]

$$\sigma_{xx}(\omega)=\frac{ie^2}{m^2\hbar}\sum_{\mathbf{k}}\sum_{i,j}\frac{|\mathbf{\Pi}^x_{ij}|^2}{\epsilon_{ij}}\left(\frac{1}{\omega+i\delta-\epsilon_{ij}}+\frac{1}{\omega+i\delta+\epsilon_{ij}}\right),$$

$$\sigma_{xy}(\omega)=\frac{ie^2}{m^2\hbar}\sum_{\mathbf{k}}\sum_{i,j}\frac{1}{\epsilon_{ij}}\left(\frac{\mathbf{\Pi}^x_{ji}\mathbf{\Pi}^y_{ij}}{\omega+i\delta-\epsilon_{ij}}-\frac{\mathbf{\Pi}^x_{ij}\mathbf{\Pi}^y_{ji}}{\omega+i\delta+\epsilon_{ij}}\right), \tag{1}$$

where i,j go over the occupied and unoccupied states, respectively ($\epsilon_{ij}=E_i-E_j$). Neglecting the small spin-flip term, the relativistic momentum operator $\mathbf{\Pi}$ can be simplified further to $-i\hbar\nabla$.[5] The conductivity is integrated over the complex energy plane by introducing a finite phenomenological inverse relaxation time, $\delta=0.5$ eV. As proposed by Oppeneer *et al.*,[7] this allows one to calculate the absorptive and dispersive parts of conductivities simultaneously without the Kramers-Kronig transformations. The special k-point method with Gaussian broadening was used for the Brillouin zone integration adopting k points in the irreducible Brillouin zone corresponding to 40 (20) meshes along each of the two (three) reciprocal lattice axes for thin films (bulk).

The magneto-optical Kerr angles can be obtained from the conductivity tensor by solving the macroscopic electromagnetic boundary problem for a given geometry. For the polar geometry in which both the magnetization and the wave vector of the incident light are perpendicular to the surface, the complex Kerr angle for the beam reflected from the surface of a magnetic material with a rotational symmetry higher than three-fold (so that the complex conductivity tensor elements satisfy $\sigma_{xx}=\sigma_{yy}$ and $\sigma_{xy}=-\sigma_{yx}$) can be expressed as a function of the photon energy ω,

$$\theta+i\varepsilon=-\frac{\sigma_{xy}}{\sigma_{xx}\sqrt{1+i4\pi\sigma_{xx}/\omega}}, \tag{2}$$

where θ and ε are the Kerr rotation and ellipticity, respectively. Note that the intraband transitions are not included in Eq. (1). So we add a Drude term, $\sigma=\sigma_0/(1+i\omega\tau)$ (with $\sigma_0=5\times10^{15}$ s^{-1}, $1/\tau=0.02$ Ry,[8]) into the diagonal element of the conductivity tensor for the determination of θ and ε.

Note that the FLAPW approach has the most accurate description of the wave functions in the interstitial region, which is of crucial importance for the determination of the conductivities and thus the MOKE spectra.[15,16] Actually we found that the interstitial plane waves gave a nontrivial contribution in the evaluation of the relativistic momentum tensor. We expect that the results provided here can serve as good references for other calculations using different band structure methods.

III. RESULTS AND DISCUSSIONS

A. fcc bulk Co

We first show the calculated polar Kerr spectra of fcc bulk Co for magnetizations along both the (001) and (111) axes in Fig. 1, accompanied by the experimental results. Our results with the intraband contributions included (thick lines) reproduce the overall features of the experimental spectra very well, except that the position of the second peak is overestimated by 0.5 eV for both the rotational angle and the ellipticity. It is obvious that the Drude term is very crucial for the determination of the MOKE spectra since, as shown by the thin dotted line in Fig. 1, the agreement between theory and experiment becomes very poor without this term. Surprisingly, our calculations indicate that the inclusion of the Drude term affects the ellipticity in a wide energy range (up to 5 eV) whereas the rotational angle is strongly altered only in the lower energy regime (<2 eV). The present results for fcc bulk Co are very similar to those given by Oppeneer *et al.* [using the augmented spherical wave (ASW) method[8]] and Guo *et al.* [using the spin-polarized relativistic linear muffin-tin orbital (SPRLMTO) method with an improvement of the atomic sphere approximation (ASA)[9]] but are quite different from that given by Gasche *et al.* (using the LMTO-ASA approach).[10] As found previously for the (001) and (110) magnetizations,[8,9] a very small deviation can be found between the MOKE spectra for the (001) and (111) magnetizations. This is expected since the magnetic anisotropy energy in this cubic system is very small.[17]

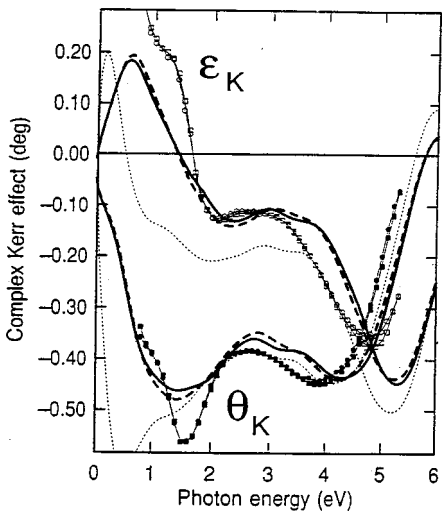

FIG. 1. The calculated and experimental results of Kerr rotation (θ_K) and ellipticity (ε_K) for fcc Co bulk. Our results including the empirical Drude conductivity are shown for two magnetization directions, (001) (thick solid curve) and (111) (thick dashed curve), while the interband spectra without Drude conductivity for (001) magnetization is also given (thin dotted curve). The curves with data points are experimental results,[11] for magnetization direction along (001) (circle) and (110) (square).

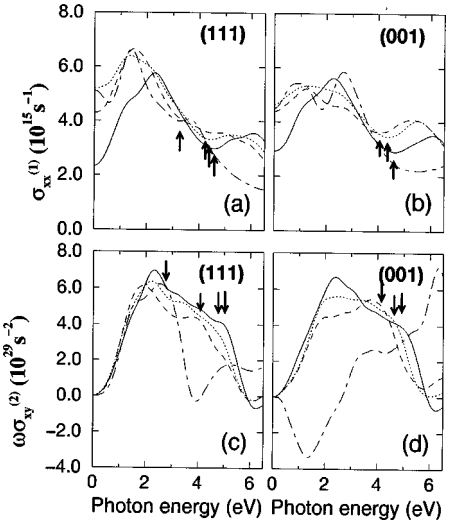

FIG. 2. The absorptive parts of the conductivity tensor of fcc free standing (111) [(a) and (c)] and (001) [(b) and (d)] Co thin films with thickness of 5 (dotted curve), 3 (dashed curve) and 1 (dot-dashed curve) atomic layers. (a) and (b) shows the real part of diagonal element $\sigma_{xx}^{(1)}$ while (c) and (d) shows the imaginary part of off-diagonal element, $\omega\sigma_{xy}^{(2)}$. Result for fcc Co bulk is also given in solid curve.

The elements of the conductivity tensor, namely, σ_{xx} and σ_{xy}, are plotted in Fig. 2. We can see that the two major peaks around 2.0 and 4.5 eV in the MOKE spectra are due to the strong peak in σ_{xy} and the dip in σ_{xx}, respectively. The change of magnetization direction slightly alters both σ_{xy} and σ_{xx}.

B. Co(001) and Co(111) ultrathin films

In previous LSDA calculations, the bulk conductivities were used to calculate the MOKE spectra. This appears to be

correct for systems with thick magnetic films since the light penetration depth in the MOKE experiments is about 100 Å, and it is known for metals that the surface effects on the electronic and magnetic properties are limited to within a few atomic layers. The surface effects on the MOKE spectra, however, have not been studied so far by means of first principles approaches. For ultrathin overlayers, this has been accounted for within a macroscopic description by adapting the bulk conductivities[15] and has provided reasonable agreement with experiment for 20 Å overlayer thickness. But this procedure fails to explain the MOKE of ultrathin films with less than 20 Å overlayer thickness—including, for example, the oscillation of the Kerr rotation with layer thickness observed widely in experiment.[18] It thus is very important to investigate the thickness dependence of the MOKE spectra in the ultrathin regime since in most practical systems nowadays the magnetic layers are reduced to a few atomic monolayers.

The optical conductivities due to the interband transitions for the Co(001) and Co(111) ultrathin films with 5, 3, and 1 atomic layers are plotted in Fig. 2. Clearly, the surface effects are very localized since the curves for three- and five-layer thick slabs are already very close to that of bulk Co. Note that due to band narrowing, the peak structures in the range 4.0–4.5 eV gradually shift towards the low-energy region as the film thickness decreases, as can be seen by the arrows pointing to the local minima of the diagonal conductivity [Figs. 2(a) and 2(b)] and the shoulders of the off-diagonal conductivity [Figs. 2(c) and 2(d)]. This indicates that if one includes the surface effects rather than using the bulk conductivity in MOKE calculations as done previously, the high energy structure in the MOKE spectra will show a redshift.

These structural changes in the optical conductivity (and thus in the MOKE spectra) due to surface effects are somewhat similar to the effects of a lattice expansion. Oppeneer *et al.*[7] reported that for Ni a larger lattice spacing causes a redshift of the high-energy peak of MOKE. Here, surface effects result in both band narrowing and an enhancement of the surface magnetic moment. (Actually, the magnetic moment of $1.65\mu_B$ for bulk Co is gradually enhanced as the thickness decreases, giving $1.70(1.75)\mu_B$, $1.77(1.81)\mu_B$, and $1.95(2.07)\mu_B$ for the (111) [(001)] free standing Co slabs with 5, 3, and 1 atomic layers, respectively. The *d* band width 5.8 eV for fcc bulk Co, is reduced to $4\sim3$ eV for the Co monolayers.) They thus cause the redshift and, meanwhile, a significant change in the magnitude of the conductivity. While the redshift occurs gradually as the film thickness decreases, the change in the magnitude of the conductivity is influenced in a more complicated way. From Figs. 2(a) and 2(b), the magnitude of the diagonal conductivity of the thin films is strongly enhanced in the low-energy region (<2 eV) compared to that for bulk Co. According to Eq. (2), this change is expected to reduce the Kerr rotation.

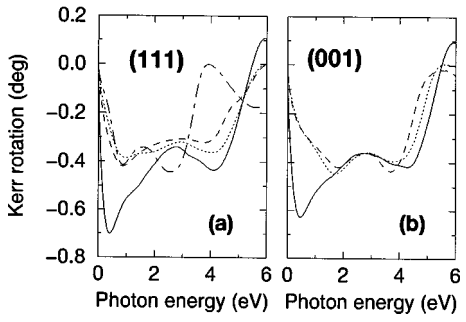

FIG. 3. The calculated Kerr rotation for fcc Co thin films with thickness of (a) 1, 3, and 5 atomic layers for (111) and (b) 3 and 5 atomic layers for (001), given together with the calculated result for fcc Co bulk for comparison; the same notation as Fig. 2 used.

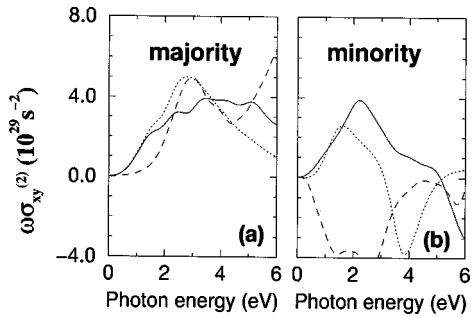

FIG. 4. The absorptive part of off-diagonal conductivity of fcc Co bulk (solid curve), (111) monolayer (dotted curve), and (001) monolayer (dashed curve) for each spin channel.

In order to see the surface effects, we give the Kerr rotation calculated from Eq. (2) for the Co thin slabs in Fig. 3, together with the bulk spectrum. Since the Drude parameters are not available for the Co slabs, the intraband term is not included for all the curves in Fig. 3. As expected, the MOKE spectra of the thin films exhibit: (i) a monotonic redshift for the high-energy peak as the thickness decreases and (ii) a reduction of the rotation angle in the low-energy region. Interestingly, these results appear to indicate that surface effects play a role similar to the Drude term and thus can be used to improve the agreement between LSDA calculations and experiment.

It is important to point out that a remarkably different result is obtained for the (001) monolayer. As can be seen in Fig. 2, the absorptive part of the off-diagonal conductivity for the Co(001) monolayer shows a very different behavior compared to the other thin films: there develops a negative peak in the low-energy region and a new positive structure in the region around 6 eV. For a more detailed analysis, we decomposed our results into contributions from the two spin parts. As shown in Eq. (1), the conductivity is given by a sum of the multiplication of two momentum operator matrix elements estimated by the relativistic spin-mixed LSDA wave functions. Clearly, it is feasible to make a spin separation for σ_{xy} and σ_{xx} when the spin-flip term is negligible.

The spin-decomposed results of the absorptive off-diagonal conductivities for the Co(001) and Co(111) monolayers and for bulk Co are given in Fig. 4. Note that the sum of the two spin channels reproduces the total off-diagonal conductivity (see Fig. 2) very well for each system, which implies that the spin-flip contribution is truly negligible. The Co(111) monolayer shows a similar profile to that of bulk Co for both spin channels, but the width of the spectrum becomes much narrower. The significant difference between the spectra for Co(001) and Co(111) suggests the sensitivity of the MOKE spectrum to changes of local symmetry and coordination number for magnetic monolayers. As expected,

TABLE I. The magnetic moments $M(\mu_B)$ and the relative SOC strength (Ref. 20) of Pt ξ for $CoPt_3$ with respect to CoPt values. Negative ξ value means that it is reduced from the value of CoPt.

	$CoPt(L1_0)$		$CoPt_3$ multilayer		$CoPt_3$ alloy	
M(Co)	1.84		1.99		1.85	
M(Pt)	0.41		0.32(0.21)		0.29	
Pt SOC	↑↑	↓↓	↑↑	↓↓	↑↑	↓↓
$\xi_{uu}^{l=1}$	1	1	−9 (%)	−9 (%)	−9 (%)	−9 (%)
$\xi_{uu}^{l=2}$	1	1	−2(%)	−1(%)	−2(%)	−1(%)
$\xi_{\dot{u}u}^{l=2}$	1	1	+4(%)	+4(%)	+4(%)	+4(%)
$\xi_{\dot{u}\dot{u}}^{l=2}$	1	1	+10(%)	+10(%)	+10(%)	+10(%)

these two monolayers give similar contributions to σ_{xy} from the majority spin part (the d band is filled so it is not so sensitive to the change of environment). The drastic difference occurs for the minority spin part; instead of giving a positive peak for other systems, a large negative peak develops in the low-energy region for the Co(001) monolayer.

C. $CoPt_n$ alloys and multilayers

Due to its large SOC strength and induced magnetic moment, Pt has been considered a good ingredient for novel magneto-optical materials and has been widely studied in compounds with $3d$ magnetic transition metals. We calculated the MOKE spectra for bulk CoPt and $CoPt_3$ alloys (with the $L1_0$ and $L1_2$ structures, respectively) and the $CoPt_3$ multilayer. The magnetization aligns along the (001) direction, and we use the experimental lattice constants[19] (for the $CoPt_3$ multilayer, the nearest Co-Pt distance is taken from the $CoPt_3$ alloys). The calculated magnetic moments and the relative SOC strength[20] of Pt, $\xi_{so}(Pt)$, with the value for CoPt as a reference, are shown in Table I for some of the dominant p and d states. As the Pt composition increases from CoPt to $CoPt_3$, the induced magnetic moment of the Pt atom ($0.41\mu_B$ in CoPt) decreases and gives close values in both the $CoPt_3$ multilayer ($0.32\mu_B$) and the $CoPt_3$ alloy ($0.29\mu_B$). The Co magnetic moment ($1.84\mu_B$ in CoPt) retains its magnitude in the $CoPt_3$ alloy but increases in the $CoPt_3$ multilayer ($1.99\mu_B$). In contrast with the magnetic moment, the SOC strength appears to be less sensitive to structural differences: as the Pt composition increases from CoPt to $CoPt_3$, the change of the Pt SOC strength reaches a maximum of 10%—but for a given set of ($l,u,\dot{u}$, spin), the same changes are found in the $CoPt_3$ alloy and multilayer. We found (not shown in Table I) that the ξ_{so}(Co) shows a negligible change ($<1\%$) in going from CoPt to $CoPt_3$.

The calculated MOKE spectra for the three systems are given in Fig. 5 and are accompanied by their experimental counterparts. We obtained a large Kerr rotation angle of up to 1° for CoPt. As the Pt composition increases, the $CoPt_3$ multilayer shows a reduction of the spectrum in the whole energy range, whereas the $CoPt_3$ alloy exhibits a new structure with two distinct peaks at 2 and 5 eV, among which the second one reaches 1°. This dependence of the MOKE spectra on the Pt composition and arrangement is somewhat similar to the results for $CoPt_n(111)$ multilayers obtained by Uba *et al.*[16] with the LMTO approach. Here, however, the amplitude of the Kerr rotation is relatively stronger.

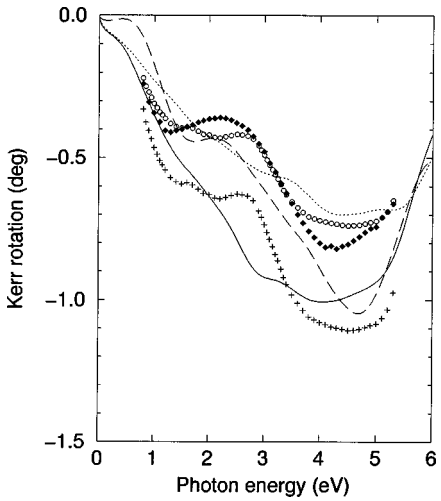

FIG. 5. The calculated and experimental results of Kerr rotation for $CoPt(L1_0)$ [solid curve: present results, open circles: experiment (Ref. 22), plus signs: experiment (given by open circles) multiplied by 1.5], $CoPt_3$ multilayer (dotted curve: present results), and $CoPt_3(L1_2)$ alloy [dashed curve: present results, filled square: experiment (Ref. 21)].

The SOC strength is known to play an important role in the determination of the Kerr rotations; a linear scaling was found for bulk transition metals.[7] For Pt-$3d$ transition metal compounds, model calculations[6,21] manipulating the SOC strength revealed that a suppression of $\xi_{so}(Pt)$ changes the MOKE spectra strongly in both their profiles and magnitudes. By contrast, a change of $\xi_{so}(Co)$ does not alter the profile of MOKE spectra but reduces their magnitudes. As seen from Fig. 5, a significant difference can be found between the MOKE spectra for the $CoPt_3$ multilayer and the $CoPt_3$ alloy, despite the fact that they have almost the same Pt SOC values (see Table I). Therefore, the structural dependence for $CoPt_3$ in our result seems to be explained by the change of band structures in the different geometries rather than the correlation between the MOKE and SOC strength mentioned above.

Compared to experiment (see Fig. 5), our results for the CoPt and $CoPt_3$ alloys show much larger values of the Kerr rotational angle. The experimental spectra exhibit a two-peak structure for both CoPt and $CoPt_3$ alloys. We obtained this feature for $CoPt_3$ alloy but not for CoPt. The discrepancies can arise because of (i) the existence of defects in the sample (ii) the unsaturated magnetization in the experiment and (iii) the use of Drude parameters of bulk fcc Co in our calculations. In addition, zero temperature is assumed in the calculations whereas the experimental data are usually taken at a higher temperature. Actually, Weller *et al.*[21] scaled their experimental data for $CoPt_3$ by a factor of 1.5 to take account of temperature effects. If the same prefactor is used for CoPt (as shown by plus signs), our result traces the measured curve quite well. For $CoPt_3$ alloy, which presents the same feature with two major peaks but different peak position and magnitude, the difference also can be attributed to the difference in the magnetization direction [the experimental results are for polar MOKE along the (111) direction].

IV. CONCLUSIONS

In summary, we performed first principles calculations of MOKE for fcc bulk Co, free standing Co(001) and Co(111) thin films, $CoPt_n$ alloys ($n=1$ and 3), and multilayer ($n=3$). We found that the anisotropy of the MOKE spectra about the (001) and (111) magnetization directions is negligible for bulk Co. The surface effects induce a redshift for the high-energy peak and reduce the Kerr rotation angle in the low-energy region due to the narrowed bandwidth and enhanced magnetization. The increase of Pt composition with respect to the CoPt layered alloy reduces the amplitude of the MOKE spectra for the $CoPt_3$ multilayer, whereas it results in a different structure of the MOKE spectra for the $CoPt_3$ alloy. This structural dependence is found to be hardly explained by the change of Pt SOC strength and its effect on the MOKE, even though the large MOKE spectra of CoPt compounds has been mainly attributed to the large Pt SOC strength.

ACKNOWLEDGMENTS

Work supported by the Office of Naval Research (Grant Nos. N00014-94-1-0030 and N00014-95-1-0489) and by grants of computer time at the NAVO Supercomputing Center and at the Arctic Region Supercomputing Center.

[1] S. D. Bader, J. Magn. Magn. Mater. **100**, 440 (1991), and references therein.

[2] K. H. J. Buschow, *Ferromagnetic Materials*, edited by E. P. Wohlfarth and K. H. J. Buschow (North-Holland, Amsterdam, 1988), Vol. 4, p. 493.

[3] P. N. Argyres, Phys. Rev. **97**, 334 (1955).

[4] H. S. Bennett and E. A. Stern, Phys. Rev. **137**, A448 (1965).

[5] C. S. Wang and J. Callaway, Phys. Rev. B **9**, 4897 (1974).

[6] H. Ebert, Rep. Prog. Phys. **59**, 1665 (1996).

[7] P. M. Oppeneer, T. Maurer, J. Sticht, and J. Kübler, Phys. Rev. B **45**, 10 924 (1992); P. M. Oppeneer, J. Sticht, T. Maurer, and J. Kübler, Z. Phys. B **88**, 309 (1992).

[8] P. M. Oppeneer, T. Kraft, and H. Eschrig, Phys. Rev. B **52**, 3577 (1995).

[9] G. Y. Guo and H. Ebert, Phys. Rev. B **50**, 10 377 (1994).

[10] T. Gasche, M. S. S. Brooks, and B. Johansson, Phys. Rev. B **53**, 296 (1996).

[11] D. Weller, G. R. Harp, R. F. C. Farrow, A. Cebollada, and J. Sticht, Phys. Rev. Lett. **72**, 2097 (1994).

[12] E. Wimmer, H. Krakauer, M. Weinert, and A. J. Freeman, Phys. Rev. B **24**, 864 (1981), and references therein; M. Weinert, J. Math. Phys. **22**, 2433 (1981).

[13] A. H. McDonald, W. E. Pickett, and D. D. Koelling, J. Phys. C **13**, 2675 (1980).

[14] J. Callaway, *Quantum Theory of the Solid State* (Academic, New York, 1991).

[15] G. Y. Guo and H. Ebert, Phys. Rev. B **51**, 12 633 (1995).

[16] S. Uba, L. Uba, N. Yaresko, A. Ya. Perlov, V. N. Antonov, and R. Gontarz, Phys. Rev. B **53**, 6526 (1996).

[17] Our recent calculations show in a very small magnetic anisotropy energy (2.1μ eV) between these two magnetizations [R.Q. Wu *et al.*, (unpublished)], a value which agrees well experiment, 1.8μ eV.

[18] Y. Suzuki and T. Katayama, in *Magnetic Ultrathin Films—Multilayers and Surfaces, Interfaces and Characterization*, MRS Symposia Proceedings No. 313, edited by B. T. Jonker *et al.* (Materials Research Society, Pittsburgh, 1993), p. 153.

[19] M. Hansen (unpublished).

[20] The SOC strength is defined as $\xi^l_{uu'}(\sigma\sigma') = (1/4c^2)\int_{r_{mt}} dr[u^\sigma_l r(\partial V_{\sigma'}/\partial r)\dot{u}^{\sigma'}_l]$, where u is a FLAPW radial functions and $\dot{u}$ its energy derivative and σ,σ' are spin indices.

[21] D. Weller, J. Sticht, G. R. Harp, R. F. C. Farrow, R. F. Marks, and H. Brändle, in *Magnetic Ultrathin Films—Multilayers and Surfaces, Interfaces and Characterization* (Ref. 18), p. 501.

[22] G. R. Harp, D. Weller, T. A. Rabedeau, R. F. C. Farrow, and R. F. Marks, in *Magnetic Ultrathin Films—Multilayers and Surfaces, Interfaces and Characterization* (Ref. 18), p. 493.